

The Effect of Symmetries and Time-Asymmetric Boundary Conditions on Entanglement in One-Dimensional Potential Scattering

N L Harshman and P Singh

Department of Computer Science, Audio Technology, and Physics, American University, 4400 Massachusetts Ave NW, Washington, DC, 20016 USA

E-mail: harshman@american.edu

Abstract. When two non-relativistic particles scatter in one dimension, they can become entangled. This entanglement is constrained by the symmetries of the system and the boundary conditions on the incoming state. Applying these constraints, three different mechanisms can be identified. Entanglement can be generated because of the superposition of reflected and transmitted modes, because (in the case of unequal masses) the wave functions are distorted by reflection, and because the scattering amplitudes vary with relative momentum and this distorts the scattered wave function. We consider three standard potentials, the hard core, Dirac delta, and double Dirac delta, and show how these mechanisms interplay. Importantly, we find that for unequal masses, neglecting the momentum variance of the wave function is a poor approximation when the reflection mode dominates.

PACS numbers: 03.67.Mn, 03.65.Nk, 03.65.Fd

1. Introduction

Before two particles scatter, they are in uncorrelated states. If we assume each particle can be described by a pure state $|\phi_i\rangle$ when the particles are far apart before the interaction, then the initial total state of the system is the product of the two one-particle states $|\phi_{in}\rangle = |\phi_1\rangle \otimes |\phi_2\rangle$. As the particles approach, the state evolves and interparticle separability is lost. Separability does not return even if the interaction is elastic and after a long time the particles are far removed beyond the interaction region. The boundary conditions of scattering are inherently time-asymmetric from the perspective of entanglement: practically, entangled particles cannot be easily prepared, and if they were, they would not approach, interact, and then emerge in a separable state. The amount of entanglement generated by scattering is constrained by symmetries. For non-relativistic scattering, free particles are associated to projective representations of the Galilean group extended by mass. Galilean invariant interactions imply conservation principles, and these shape the mechanisms by which the entanglement occurs.

For simplicity, we consider the generation of entanglement in the non-relativistic scattering of two structureless, distinguishable particles in one dimension. Within this limited context, we show that the constraints of symmetry and time-asymmetric boundary conditions on the incoming state imply that scattering entanglement proceeds by the combination of three mechanisms. The simplest is the entanglement between transmission and reflection. This kind of entanglement is also the coarsest, because as long as the transmitted and reflected modes are orthogonal, each particle can effectively be thought of as two-level system corresponding to different sides of the interaction region. The other two mechanisms create entanglement by distorting the mode wave functions in a non-separable fashion. If particles have different masses, reflection (the reversal of the relative momentum) creates entanglement from wave function distortion in the reflected mode. Finally, the wave function of the out-going state will be distorted inseparably because the scattering amplitudes vary with the relative momentum. This kind of entanglement diminishes as each particle's wave function becomes sharply peaked about a central value, but the entanglement due to reflection does not.

The study of how entanglement is generated in scattering has interest for a variety of reasons. Some leading possibilities for practical implementations of quantum information processes, such as ultracold atoms and some solid state devices, are physical systems where scattering is central to the dynamics. The quantum information theory of systems with continuous variables and mixed continuous-discrete variables has many open questions, and scattering systems provide rich structure for exploration of these systems. Finally, scattering is a fundamental method of interaction for systems at all quantum scales, and one could hope that entanglement might provide new perspective on this basic interaction process.

Entanglement generation in non-relativistic scattering of structureless, distinguishable particles has been considered previously [1, 2, 3, 4, 5, 6, 7, 8, 9]. Most of these

previous treatments consider interactions of a single species [2, 4, 5, 6, 7, 9], and have focused on particular special cases. This article provides a unified treatment of all these results and provides a framework for further exploration and generalization. Specifically, it applies methods described in [10] to three finite-range potentials: hard core, Dirac delta, and double Dirac delta.

2. Entanglement and scattering boundary conditions

For two structureless, distinguishable, non-relativistic particles in one-dimension, the momentum operators of each particle $\{\hat{P}_1, \hat{P}_2\}$ form a complete set of commuting observables (CSCO). A tensor product structure corresponding to this CSCO is $\mathcal{H}_1 \otimes \mathcal{H}_2$, where \mathcal{H}_i is the single, free-particle Hilbert space. Then, a pure state of the system is described by the bi-momentum wave function $\phi(p_1, p_2)$. For simplicity, we will restrict considerations so that $\phi(p_1, p_2) \in \mathcal{S}(\mathbb{R}^2)$, the Schwartz space on the bi-momentum plane (p_1, p_2) . This means that we consider wave functions that are smooth, infinitely differentiable, and rapidly decreasing at infinity. With this mild and physically reasonable restriction, we can employ Riemann integrals and be assured of their finiteness.

The interparticle entanglement can be calculated from $\phi(p_1, p_2)$ using the purity of the reduced density matrix [10]:

$$p_{12}(\phi) = \int dp_1 dp_2 dp'_1 dp'_2 \phi(p_1, p_2) \phi^*(p'_1, p'_2) \phi(p'_1, p'_2) \phi^*(p_1, p'_2). \quad (1)$$

The interparticle purity p_{12} is an entanglement monotone (more purity always mean less entanglement) and takes values in the interval $(0, 1]$ as long as the wave function $\phi(p_1, p_2)$ is normalized. For continuous variable entanglement, the purity is useful because, unlike the entropy of entanglement, one does not need to diagonalize the reduced density matrix. Additionally, the simple form (1) allows for analytic results in certain cases (see below).

Without loss of generality, all calculations can be performed in the center-of-mass (COM) reference frame where the expectation value of the total momentum operator $\hat{P} = \hat{P}_1 \otimes \hat{\mathbb{I}}_2 + \hat{\mathbb{I}}_1 \otimes \hat{P}_2$ in the state $\phi_{in}(p_1, p_2)$ is zero. Galilean transformations, including global boosts and translations, are represented by unitary transformations that are local with respect to the interparticle tensor product structure $\mathcal{H}_1 \otimes \mathcal{H}_2$ and therefore do not affect the value of the interparticle entanglement [11]. In other words, the operator that performs the boost to the COM frame factors as $U(-\langle \hat{P} \rangle) = U_1(-\langle \hat{P} \rangle) \otimes U_2(-\langle \hat{P} \rangle)$. The value $\langle \hat{P} \rangle$ is invariant under the dynamics as long as the interaction is Galilean invariant.

One boundary condition of a scattering experiment is that the in-state ϕ_{in} (formally the state in the limit $t \rightarrow -\infty$) is separable with respect to the interparticle tensor product structure. Since $\phi_{in}(p_1, p_2) = \phi_{in,1}(p_1) \phi_{in,2}(p_2)$, one calculates that $p_{12}(\phi_{in}) = 1$ for every scattering system.

Another boundary condition for scattering is that the particle wave functions represent states that are “incoming” before the scattering. If the interaction potential has finite range, “incoming” suggests that the single-particle position expectation values in the in-state are on opposite sides of the potential region. Assuming the COM reference frame, the single-particle momentum expectation values are equal in magnitude and directed toward the potential region. Further, before the interaction the position wave function should have no (or essentially no) support in the potential region and the momentum wave functions have support only (or essentially only) on the positive semi-axis for one particle and on the negative semi-axis for the other. For our calculations, we consider the product of two Gaussian wave packets:

$$\phi_{in}^G(p_1, p_2) = N_1 N_2 e^{ip_1 a_1} e^{-\frac{(p_1 - k)^2}{4\sigma_1^2}} e^{ip_2 a_2} e^{-\frac{(p_2 + k)^2}{4\sigma_2^2}}, \quad (2)$$

where $N_i = (2\pi\sigma_i^2)^{-1/4}$, k is the magnitude of the momentum of each particle in the COM frame, a_i are the central positions, and σ_i are the momentum uncertainties for each particle’s Gaussian. As long as $a_1 = -a_2$ is large and if $k/\sigma_i \ll 1$, this wave function satisfies at least these heuristic notions of incoming.

A more refined notion of incoming boundary conditions is the Hardy space hypothesis of A. Bohm and collaborators [12]. In that formulation, further restrictions are placed on the space of allowable in-states, which are defined by the preparation apparatus, such as an accelerator. An alternate CSCO for two particle elastic scattering is $\{\hat{P}, \hat{W}, \hat{\Xi}\}$ with generalized eigenvalues of the total momentum $p \in \mathbb{R}$, the internal energy $w \in \mathbb{R}^+$, and relative momentum direction $\chi = \pm$, respectively. Then the incoming wave function $\phi_{in}(p, w, \chi)$ is a Hardy function from below in internal energy, i.e. it is the boundary value on the real semi-axis of a function that is analytic in the lower-half complex plane when w is extended to complex values. Additionally, the wave functions are Schwartz, giving them well-behaved smoothness and convergence properties in the internal energy and the total momentum. Conjugate requirements apply to the wave functions that represent the out-observables, which are defined by the detectors, but these do not enter the present analysis. It is an open question as to whether the requirements of the Hardy space hypothesis are consistent with the separability constraint on the in-state described above. However, since the Hardy-Schwartz spaces are dense in the Hilbert space, there will always be elements as close to separable as would be physically indistinguishable.

We will not consider the intricacies of the time-dependence of the scattering entanglement. Instead, since the in-state particles are always unentangled, any entanglement in the final out-state will have been generated in the scattering event. The out-state (formally the state in the limit $t \rightarrow +\infty$) is found by

$$\phi_{out} = \hat{S} \phi_{in}, \quad (3)$$

where \hat{S} is the scattering operator. The exact form of the S-operator can be calculated for finite-range potentials by transforming to the COM-relative momentum coordinate

system

$$\begin{aligned} p &= p_1 + p_2 \\ q &= \mu_2 p_1 - \mu_1 p_2, \end{aligned} \tag{4}$$

where $\mu_i = m_i/(m_1 + m_2)$ and solving the time independent Schrödinger equation in the relative momentum variable q . The S-matrix in the (p, q) -basis of the CSCO $\{\hat{P}, \hat{Q}\}$ is

$$\langle p, q | \hat{S} | p', q' \rangle = \delta(p' - p) (t(q)\delta(q - q') + r(q)\delta(q + q')) \tag{5}$$

The functions $t(q)$ and $r(q)$ are the transmission and reflection amplitudes and unitarity implies $|t(q)|^2 + |r(q)|^2 = 1$. We also note in passing that the S-operator is a local operator with respect to the tensor product structure dictated by the CSCO $\{\hat{P}, \hat{Q}\}$, and so entanglement with respect to that tensor product structure is dynamically invariant [13], i.e. $p_{pq}(\phi_{in}) = p_{pq}(\phi_{out})$.

Using (5) and transforming back to the CSCO $\{\hat{P}_1, \hat{P}_2\}$, the out-state can be expressed as the sum of a transmitted and a reflected mode

$$\phi_{out}(p_1, p_2) = \phi_{tra}(p_1, p_2) + \phi_{ref}(p_1, p_2) \tag{6}$$

where

$$\phi_{tra}(p_1, p_2) = t(\mu_2 p_1 - \mu_1 p_2) \phi_{in}(p_1, p_2) \tag{7}$$

and

$$\phi_{ref}(p_1, p_2) = r(\mu_2 p_1 - \mu_1 p_2) \phi_{\overline{in}}(p_1, p_2). \tag{8}$$

The wave function $\phi_{\overline{in}}(p_1, p_2)$ is the in-state wave function $\phi_{in}(p_1, p_2)$ as transformed by the reflection of the internal momentum $q \rightarrow -q$. One can show

$$\phi_{\overline{in}}(p_1, p_2) = \phi_{in}(\bar{p}_1, \bar{p}_2) \tag{9}$$

where (\bar{p}_1, \bar{p}_2) are

$$\begin{aligned} \bar{p}_1 &= (\mu_1 - \mu_2)p_1 + 2\mu_1 p_2 \\ \bar{p}_2 &= 2\mu_2 p_1 + (\mu_2 - \mu_1)p_2. \end{aligned} \tag{10}$$

Note that this transformation of momentum variables typically distorts the shape of the wave function and disrupts separability (see Figure 1). However, for the case of equal masses $\mu_1 = \mu_2 = 1/2$, we find $(\bar{p}_1, \bar{p}_2) \rightarrow (p_2, p_1)$ and so the function $\phi_{\overline{in}}(p_1, p_2) \rightarrow \phi_{in}(p_2, p_1)$ is still separable (although the reflected state as a whole is still generally inseparable because of the factor of $r(q)$).

The reflected Gaussian wave function $\phi_{in}^G(p_1, p_2)$ will in addition be separable if

$$m_1/\sigma_1^2 = m_2/\sigma_2^2, \tag{11}$$

a relationship first noted by Schulman [1]. More generally, an analytic expression for the purity $p_{12}(\phi_{in}^G(p_1, p_2))$ exists [10]:

$$p_{12}(\phi_{in}^G) = \frac{\sigma_1 \sigma_2}{\sqrt{((\mu_1 - \mu_2)^2 \sigma_1^2 + 4\mu_1^2 \sigma_2^2)(4\mu_2^2 \sigma_1^2 + (\mu_2 - \mu_1)^2 \sigma_2^2)}}. \tag{12}$$

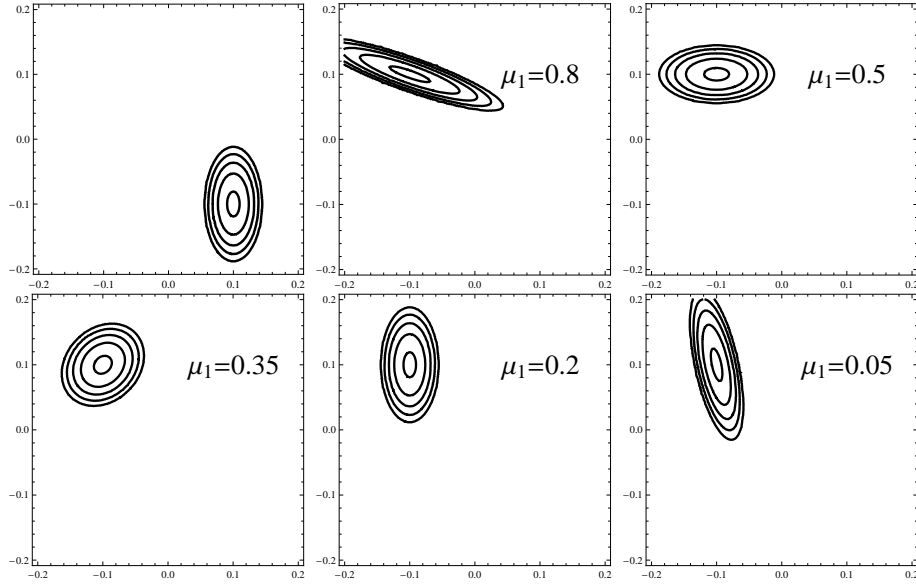


Figure 1. These contour plots depict the bi-momentum probability densities $|\phi_{in}^G(p_1, p_2)|^2$ (upper, left subfigure) and $|\phi_{inbar}^G(p_1, p_2)|^2$ (the rest) for various values of the mass fraction $\mu_1 = m_1/(m_1 + m_2)$ plotted on the (p_1, p_2) plane. For each graph, the central momentum is $k = 0.1$ and the momentum variances are $\sigma_1 = k/10$ and $\sigma_2 = k/5$. As the contours move outwards, each represents a reduction of probability density by a factor of 10. Unless the major and minor axes of the ellipses align with the (p_1, p_2) -axes, the wave function has interparticle entanglement.

Alternatively, using $\mu_2 = 1 - \mu_1$ and the ratio $c = \sigma_2/\sigma_1$, this can be re-expressed as

$$p_{12}(\phi_{in}^G) = \frac{c}{\sqrt{((2\mu_1 - 1)^2 + 4\mu_1^2 c^2)(4(1 - \mu_1)^2 + (1 - 2\mu_1)^2 c^2)}}. \quad (13)$$

This function takes a maximum value of 1 when either $m_1 = m_2$ or $m_1/\sigma_1^2 = m_2/\sigma_2^2$ (see Figure 2). For this particular combination of constants, the terms in the exponential that are proportional to the product $p_1 p_2$ all cancel out and $\phi_{in}^G(p_1, p_2)$ is again a product of Gaussians in p_1 and p_2 , except the variance (σ_1, σ_2) switch roles to (σ_2, σ_1) when $m_1 = m_2$. When $m_1/\sigma_1^2 = m_2/\sigma_2^2$, we find (σ_1, σ_2) are unchanged under reflection.

The wave functions $\phi_{tra}(p_1, p_2)$ and $\phi_{ref}(p_1, p_2)$ are orthogonal modes. The domain of support for $\phi_{in}(p_1, p_2)$ (and therewith $\phi_{tra}(p_1, p_2)$) can be chosen without loss of generality as the region where $p_1 > 0$ and $p_2 < 0$. The domain of support of $\phi_{inbar}(p_1, p_2)$ (and therewith $\phi_{ref}(p_1, p_2)$) is then the region where $(\mu_1 - \mu_2)p_1 + 2\mu_1 p_2 > 0$ and $2\mu_2 p_1 + (\mu_2 - \mu_1)p_2 < 0$. Remembering $\mu_2 = 1 - \mu_1$ and $1 > \mu_1 > 0$, one can show these domains have no intersection. Since the domains of support of the transmitted and reflected states are disjoint, the purity of the out-state is the sum of the purities of those two modes:

$$p_{12}(\phi_{out}) = p_{12}(\phi_{tra}) + p_{12}(\phi_{ref}) \quad (14)$$

From this observation, two kinds of entanglement can be identified. One source of entanglement is the superposition of the transmitted and reflected modes. The other

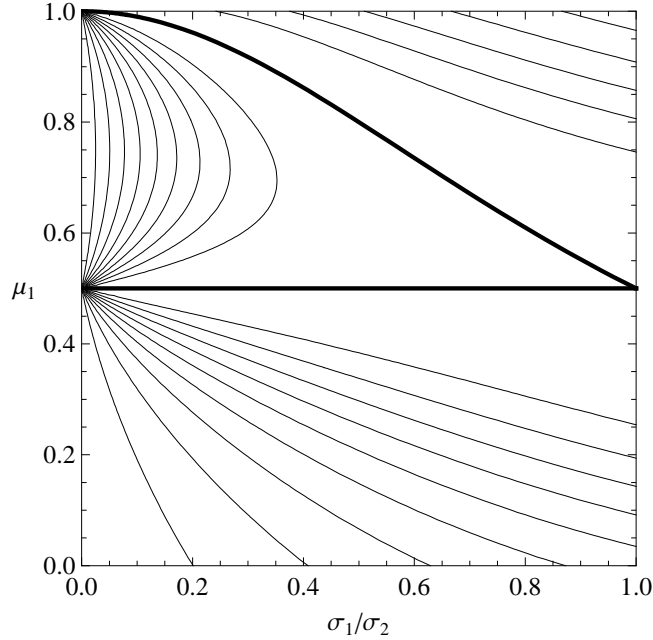


Figure 2. This contour plot depicts the values of the function $p_{12}(\phi_{in}^G)$ (13). The thick contours trace the two lines of maximum purity, corresponding to the values of μ_1 and σ_2/σ_1 where the Gaussian bi-momentum wave function is separable even after the reflection $q \rightarrow -q$. Each subsequent contour represents a purity reduction of 0.1.

is the entanglement within the transmitted and reflected modes themselves. Since the transmission and reflection amplitudes depend on p_1 and p_2 in a non-factorizable way through the variable q , those modes typically have shapes that are distorted in a non-separable way, and the act of reflection contributes additional distortion.

One useful approximation applies when $t(q)$ and $r(q)$ are approximately constant over the primary support of the two-particle momentum modes. The expectation value for the relative momentum the in-state in the COM frame equal is k , so in this approximation one finds the transmission probability is $|t(k)|^2$ and reflection probability is $|r(k)|^2$. For the transmitted state, one calculates

$$p_{12}(\phi_{tra}) = |t(k)|^4 \quad (15)$$

and for the reflected state one calculates

$$p_{12}(\phi_{ref}) = |r(k)|^4 p_{12}(\phi_{in}). \quad (16)$$

For the equal mass case (or for Gaussian states when the Schulman condition (11) is satisfied) the constant amplitude approximation reduces to

$$p_{12}(\phi_{out}) = |t(k)|^4 + |r(k)|^4. \quad (17)$$

For Gaussian in-states like (2), we find

$$p_{12}(\phi_{out}) = |t(k)|^4 + |r(k)|^4 p_{12}(\phi_{in}^G). \quad (18)$$

Because $p_{12}(\phi_{\overline{in}}) < 1$, this approximation (18) is always less than the coarsest approximation (17); reflection distortion can only increase entanglement in this approximation.

3. Results for specific potentials

The following subsections make explicit calculations of entanglement for specific potentials and a variety of in-state distributions. For all results, we calculate in the COM frame and assume the in-state has the form (2). This means that the in-state can be fully described by five parameters: m_1 , m_2 , k , σ_1 , and σ_2 . Instead of m_1 and m_2 , the following results will use $\mu_1 = m_1/M$ and the total mass variable $M = m_1 + m_2$.

3.1. Hard core potential

This is the simplest case of potential scattering. In the relative variable $x = x_1 - x_2$, the potential has the form

$$V(x) = \begin{cases} 0 & x > 0 \\ \infty & x \leq 0 \end{cases} \quad (19)$$

Solving the Schrödinger equation in the relative momentum gives the trivial answer $r(q) = -1$ and $t(q) = 0$ for all q . For this potential, with equal masses, the coarsest approximation (17) would suggest that a long time after hard core scattering there is no entanglement, and this result is reported in [4]. However, as noted in [3, 8] and confirmed by these calculations, reflection can cause distortion and the expression (18) is exact since

$$p_{12}(\phi_{out}) = p_{12}(\phi_{ref}) = p_{12}(\phi_{\overline{in}}). \quad (20)$$

Figures 1 and 2 can therefore also be considered as depicting the entangling effects of hard core scattering. Note that this entanglement is not dependent on any absolute scale such as the energy, momentum, mass, but depends on the ratios of masses and variances. This kind of entanglement due to reflection (which is a factor in other potential scattering results below) does not disappear in the narrow wave packet approximation even though the scattering amplitudes are slowing varying or not varying at all. This kind of entanglement due to momentum distribution correlations within a single mode can be expected to be difficult to measure. For direct measurement, one would need a device to measure the momentum distribution of the scattered particles that at least has a resolution smaller than the in-state momentum variances.

3.2. Dirac delta potential

This potential has the form

$$V(x) = \alpha\delta(x). \quad (21)$$

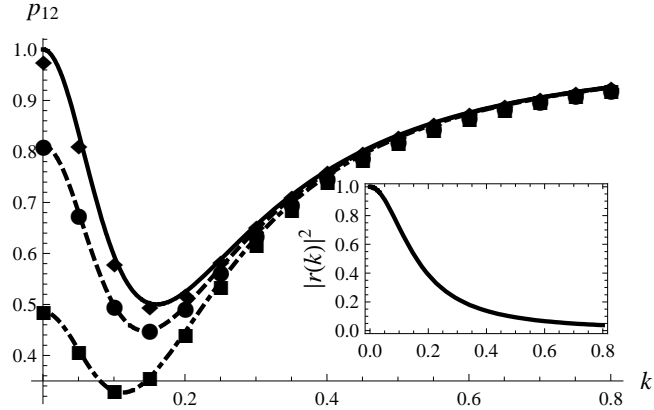


Figure 3. The data points on the main plot depict the function $p_{12}(\phi_{out}^G)$ and two of its analytic approximations for the case $m_2 = 4m_1$ for the Dirac delta potential. On the horizontal axis, the central momentum of the wave function k is measured in units of $\alpha(m_1 + m_2)/\hbar^2$. The black line is the coarse two-mode approximation (17) that is independent of σ_1/σ_2 . This line also equals the two-mode approximation with reflection distortion (18) for the Schulman condition (11) case $\sigma_1/\sigma_2 = 1/2$. The dashed line is (18) for $\sigma_1/\sigma_2 = 1$ and the dot-dashed line is (18) for $\sigma_1/\sigma_2 = 1$. The diamonds, circles and squares are the exact result computed numerically for $(\sigma_1 = k/10, \sigma_2 = k/5)$, $(\sigma_1 = k/5, \sigma_2 = k/5)$, and $(\sigma_1 = k/5, \sigma_2 = k/10)$, respectively.

The reflection amplitude is

$$r(q) = \frac{i}{\frac{k\hbar^2}{\alpha\mu} - i} = \frac{i}{\frac{k\hbar^2}{\alpha M\mu_1(1-\mu_1)} - i} \quad (22)$$

and the transmission amplitude is $t(q) = 1 + r(q)$, where μ is the reduced mass $\mu = \mu_1\mu_2 M$. This potential has no resonances, and since the single bound state that occurs when $\alpha < 0$ does not participate in the elastic scattering, we can replace $\alpha \rightarrow |\alpha|$ without affecting any scattering entanglement results. This potential is considered in [2, 6, 9] for the equal mass case.

To highlight the distinction between the exact result for the purity and the two-mode approximation (17) and two-mode with reflection approximation (18), consider Figure 3 which depicts to particles scattering via the Dirac delta interaction when $m_2 = 4m_1$. The figure reveals that when the particles have different masses, the relative momentum variance σ_1/σ_2 dramatically effects the entanglement. Unless, the Schulman condition (11) is fulfilled, the entanglement is enhanced by this mechanism for small central momentum k . For low k , reflection dominates the scattering (see Figure 3 inset showing reflection probability $|r(k)|^2$) and therefore the entangling distortion of the wave function due to reversal of q is prominent. Generally, the maximum entanglement (minimum purity) occurs at a value of k where the transmission and reflection probabilities are equal, but the location of the extreme shifts to lower k due to this reflection distortion, which for a given mass ratio, depends only σ_1/σ_2 . Also note that in Figure 3, the approximation (18) that incorporates reflection entanglement and the numerical evaluation of the exact result (14) are very close even for relatively wide

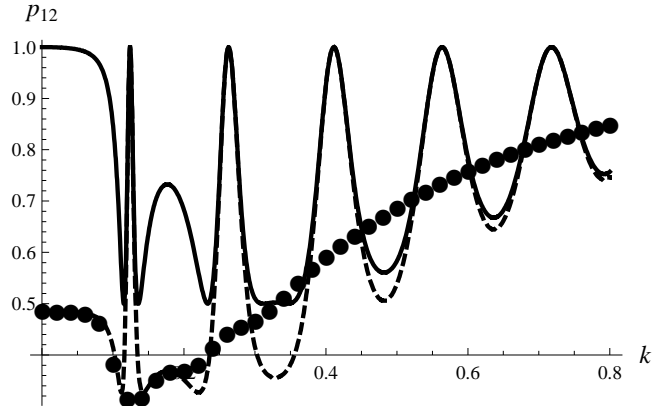


Figure 4. The data points on the main plot depict the function $p_{12}(\phi_{out}^G)$ and two of its approximations for the case $m_2 = 4m_1$ for the double Dirac delta potential. On the horizontal axis, the central momentum of the wave function k is measured in units of $\alpha(m_1 + m_2)/\hbar^2$. The black line is the coarse two-mode approximation (17) that is independent of σ_1/σ_2 and the dashed line is (18) for $\sigma_1/\sigma_2 = 2$. The circles are the exact result computed numerically for $\sigma_1 = k/5$.

Gaussian wave functions $\sigma_i/k = 1/5$. In the next example, the scattering amplitudes vary with k at a faster rate and this will no longer always be true.

3.3. Double Dirac delta potential

This potential has the form

$$V(x) = \alpha (\delta(x + a) + \delta(x - a)). \quad (23)$$

The transmission amplitude is

$$t(q) = \frac{q^2/b^2}{(e^{4iaq} - 1) + 2iq/b + q^2/b^2} \quad (24)$$

and $r(q) = t(q) - 1$ where $b = (m_1 + m_2)\alpha/\hbar^2$. This potential has resonant transmission $|t(q)|^2 = 1$ for particular values of the relative momentum q . For plots below, we choose $a = 10b^{-1}$ and measure q in units of b . This case is considered in [5] for equal mass particles, and our methods clarify those results about the relative widths of resonances and the wave functions.

In Figure 4, we contrast the two approximations and the numerically-evaluated exact results for $m_2 = 4m_1$ and $\sigma_1 = k/5$ and $\sigma_2 = k/10$, and Figure 5 looks at this region around the first, narrowest resonance in more detail for a variety of absolute scales for the variances, but the same fixed ratio of variances $\sigma_1/\sigma_2 = 2$. At resonance, the purity of both approximations become unity because only the transmission mode contributes. The variance of the wave functions generally has the effect of smoothing out the rapid variations of the approximations. However, in agreement with [5], we also see a slight enhancement of entanglement (reduction of purity) for wave functions wider than the narrow resonance. As the variance scale get smaller, this effect disappears, and the

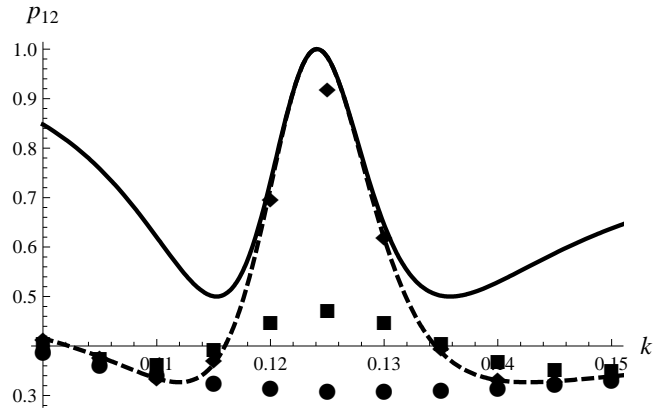


Figure 5. This depicts an enlargement of Figure 4 around the first transmission resonance. The circles, squares, and diamonds are the exact result computed numerically for $\sigma_1/\sigma_2 = 2$ with different variance scales $\sigma_1 = k/5$, $\sigma_1 = k/10$, and $\sigma_1 = k/50$, respectively.

exact results become closer and closer to the two-mode with reflection approximation (18). Note that even as the wave functions become narrower, the coarsest two-mode approximation (17) consistently underestimates the entanglement; entanglement due to reflection is independent of the scale of the variances and only depends on the masses and the ratio of the variances. Also note that because of convolution with a fast-varying scattering amplitude, some narrow wave functions will become more entangled than wider wave functions.

4. Conclusion

In summary, by employing symmetry methods and applying the time asymmetric boundary conditions, the problem of scattering entanglement in one dimension can be analyzed by the relative importance of three different mechanisms: two-mode superposition, reflection distortion, and scattering amplitude distortion.

The overall momentum dependence of the entanglement is determined on a coarse scale by the two-mode effect, but if one could measure the momentum distributions of the two particle in the out-state, then further entanglement would be detected. The entanglement due to reflection is intriguing because it depends on the ratio of the particle masses and the ratio of the momentum variances. The effect is most pronounced when the more massive particle has a more certain momentum. No matter how sharp the initial momentum distribution are, quantum correlations ensue for Gaussian states unless the Schulman condition is satisfied or the masses are equal. As the distribution gets narrower, however, it would also become more difficult to measure this entanglement. Scattering amplitudes that vary rapidly with relative momentum on the scale of the variances also distort the wave function in an inseparable manner, and this kind of entanglement becomes less prominent for narrow momentum distributions.

More complicated scattering problems must be considered if these methods will be useful for practical applications to quantum information processes with cold atoms and solid state devices. Generally, these will require multi-dimensional results for particles with spin (although some one-dimensional scattering may have applications; see [14] for an example). In addition to possible other new effects, these three mechanisms will continue to apply to these situations. The application of symmetry methods and the restriction of time-asymmetric boundary conditions remain valid, and they will be the starting point for future work on this topic.

Acknowledgments

The authors would like to acknowledge the Research Corporation for supporting this research through a Cottrell College Science Award. They also would like thank A. Patch, S. Wickramasekara, Y. Strauss and I. Antoniou for useful discussions and the organizers of 5th International Symposium of Quantum Theory and Symmetries in Valladolid Spain in July 2007 for their hard work and hospitality (especially M. Gadella, F. Gómez-Cubillo, and S. Kuru).

References

- [1] Schulman LS 1998 *Phys. Rev. A* **57** 840
- [2] Mack H and Freyberger M 2002 *Phys. Rev. A* **66** 042113
- [3] Schulman LS 2004 *Phys. Rev. Lett.* **92** 210404
- [4] Law CK 2004 *Phys. Rev. A* **70** 062311
- [5] Tal A and Kurizki G 2005 *Phys. Rev. Lett.* **94** 160503
- [6] Wang J, Law CK, and Chu MC 2005 *Phys. Rev. A* **72** 022346
- [7] Wang J, Law CK, and Chu MC 2006 *Phys. Rev. A* **73** 034302
- [8] Schmüser F and Janzing D 2006 *Phys. Rev. A* **73** 052313
- [9] Bußhardt M and Freyberger M 2007 *Phys. Rev. A* **75** 052101
- [10] Harshman NL and Hutton G 2007 Entanglement Generation in the Scattering of One-Dimensional Particles *Preprint* arXiv:0710.5776
- [11] Harshman NL and Wickramasekara S 2007 *Open Sys. Inf. Dyn.* **14** 341
- [12] Bohm A, Antoniou I and Kielanowski P 1994 *Phys. Lett. A* **189** 442
Bohm A, Maxson S, Loewe M 1997 and Gadella M *Physica A* **236** 485
Bohm A 1999 *Phys. Rev. A* 861
- [13] Harshman NL and Wickramasekara S 2007 *Phys. Rev. Lett.* **98** 080406
- [14] Buscemi F, Bordone P and Bertoni A 2006 *Phys. Rev. A* **73** 052312